

1. Abstract

Filtration of feed containing multiple species of particles is a common process in the industrial setting. In this work we propose a model for filtration of a suspension containing an arbitrary number of particle species, each with different affinities for the filter membrane. We formulate a number of optimization problems pertaining to effective separation of desired and undesired particles in the special case of two particle species, and we present results showing how properties such as feed composition affect the optimal filter design (internal pore structure). To make our model suitable for filter design application (pore shape optimization) of feed containing arbitrary number of particle species, we propose new objective function (fast method) based on the quantities evaluated at early stage of the filtration. In addition, we propose a novel multi-stage filtration strategy, which provides a significant mass yield improvement for the desired particles, and surprisingly higher purity of the product as well.

2. Mathematical Model

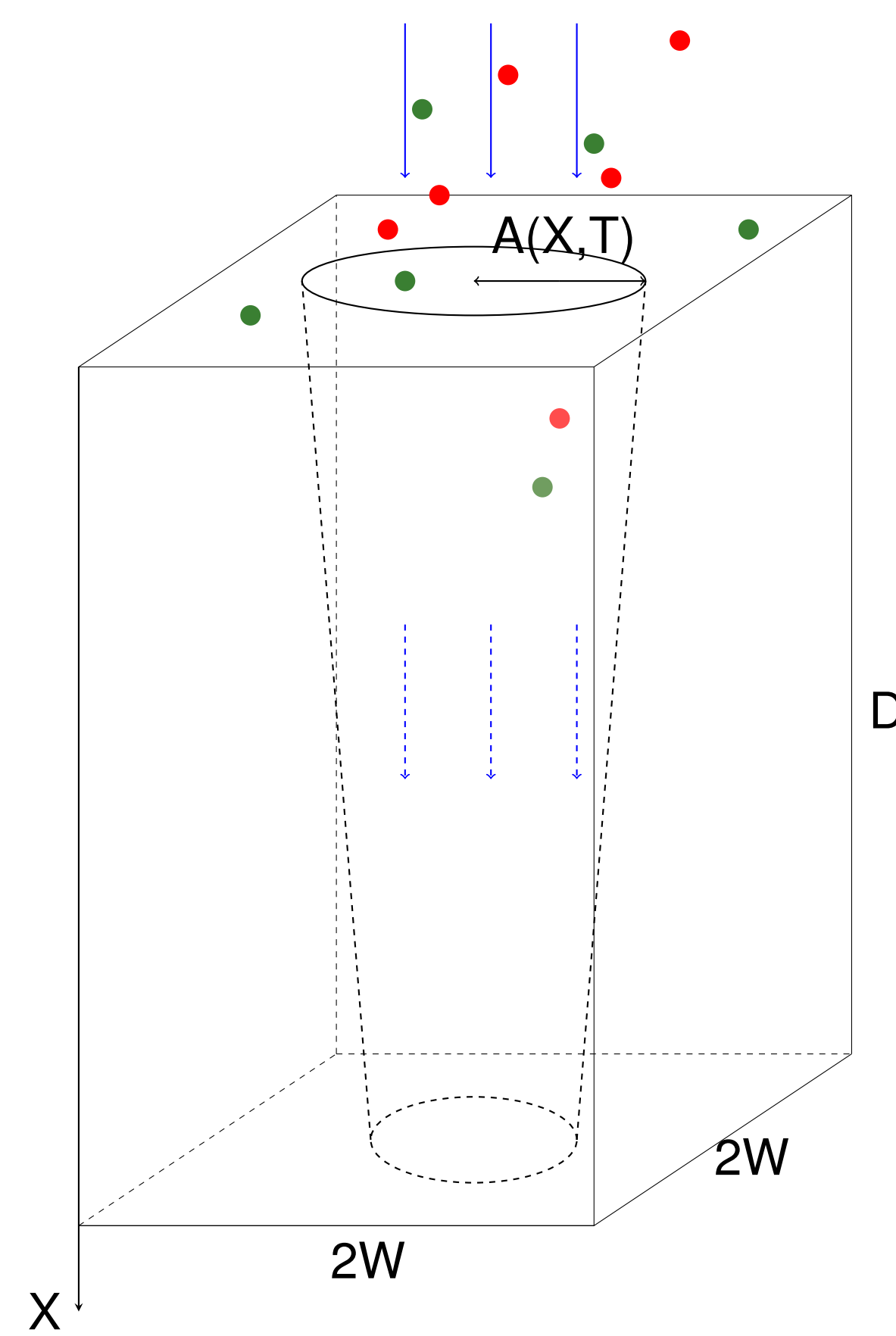


Figure 1: Sketch of a cylindrical pore inside unitary prism, representing a basic building-block of the filter membrane. Blue arrows indicate the flow direction and colored dots indicate the different particle types present in the feed.

We consider dead-end filtration of a feed solution containing two types (different physicochemical properties) of particles, type 1 and type 2, through a planar membrane filter under constant pressure. We assume that the membrane is composed of identical pores of circular cross-section with radius $A(X, T)$ (where X is distance along the pore axis), periodically repeating in a square lattice arrangement. Each pore is contained in a unit prism with square base $2W \times 2W$ and height D (see Fig. 1), where $W \ll D$. The incompressible feed (assumed Newtonian with viscosity μ) flows through the pore with cross-sectionally averaged axial velocity, $U_p(X, T)$, given in terms of the pressure $P(X, T)$ by

$$U_p(X, T) = -\frac{K_p(X, T)}{\mu} \frac{\partial P}{\partial X}, \quad (1)$$

where $K_p = A^2(X, T)/8$ is the local permeability of an isolated pore. This is equivalent to a Darcy flow model with velocity $U(T)$ within the membrane related to $U_p(X, T)$ via porosity $\Phi_m = \pi A^2(X, T)/(2W)^2$,

$$U(T) = \Phi_m U_p(X, T) = -\frac{K(X, T)}{\mu} \frac{\partial P}{\partial X}, \quad (2)$$

where

$$K(X, T) = \frac{\pi A(X, T)^4}{32W^2} \quad (3)$$

is the membrane permeability. The flow is driven by constant pressure drop P_0 across the membrane. Conservation of mass then closes the model, giving the equation and boundary conditions governing the pressure $P(X, T)$ within the membrane as

$$\frac{\partial}{\partial X} \left[K(X, T) \frac{\partial P}{\partial X} \right] = 0, \quad 0 \leq X \leq D, \quad (4)$$

$$P(0, T) = P_0, \quad P(D, T) = 0. \quad (5)$$

Extending the approach of Sanaei & Cummings [2; 3], we propose the following fouling model equations, which assume that the two particle types are transported independently by the solvent and do not interact:

$$U_p \frac{\partial C_i}{\partial X} = -\Lambda_i \frac{C_i}{A}, \quad C_i(0, T) = C_{0i}, \quad i = 1, 2, \quad (6)$$

$$\frac{\partial A}{\partial T} = -\sum_{i=1,2} \Lambda_i \alpha_i C_i, \quad A(X, 0) = A_0(X), \quad (7)$$

where $C_i(X, T)$ is the concentration (mass per unit volume of solution) of type i particles; Λ_i is a particle deposition coefficient for type i particles; and α_i is an unknown (problem-dependent) constant related inversely to the density of the material that comprises type i particles. Equation (7) assumes the rate of pore radius shrinkage (due to the particle deposition) is a linear function of the local particle concentrations at depth X , and derives from a mass-balance of the particles removed from the feed, consistent with (6).

3. Results

3.1 Definitions for filter performance evaluation and optimization

Metric	Description	Range/definition
$u(t)$	flux	$(0, \infty)$
$j(t)$	throughput	$= \int_0^t u(\tau) d\tau$
$j(t_f)$	total throughput at final time t_f	$= \int_0^{t_f} u(\tau) d\tau$
$c_{i,ins}(t)$	instantaneous concentration at the outlet for each particle type i	$(0, c_i(0, t))$
$c_{i,acm}(t)$	accumulative concentrations of each particle type i in the filtrate	$(0, c_i(0, t))$
$R_i(t)$	instantaneous particle removal ratio for type i particles	$[0, 1]$
$\bar{R}_i(t)$	cumulative particle removal ratio for type i particles	$[0, 1]$
k_i	purity for type i particles in the filtrate at the end of filtration	$[0, 1]$
γ	effective physicochemical difference between the two species	$[0, 1]$

3.2 Effect of particle composition ratio ξ on optimization with fast and slow method

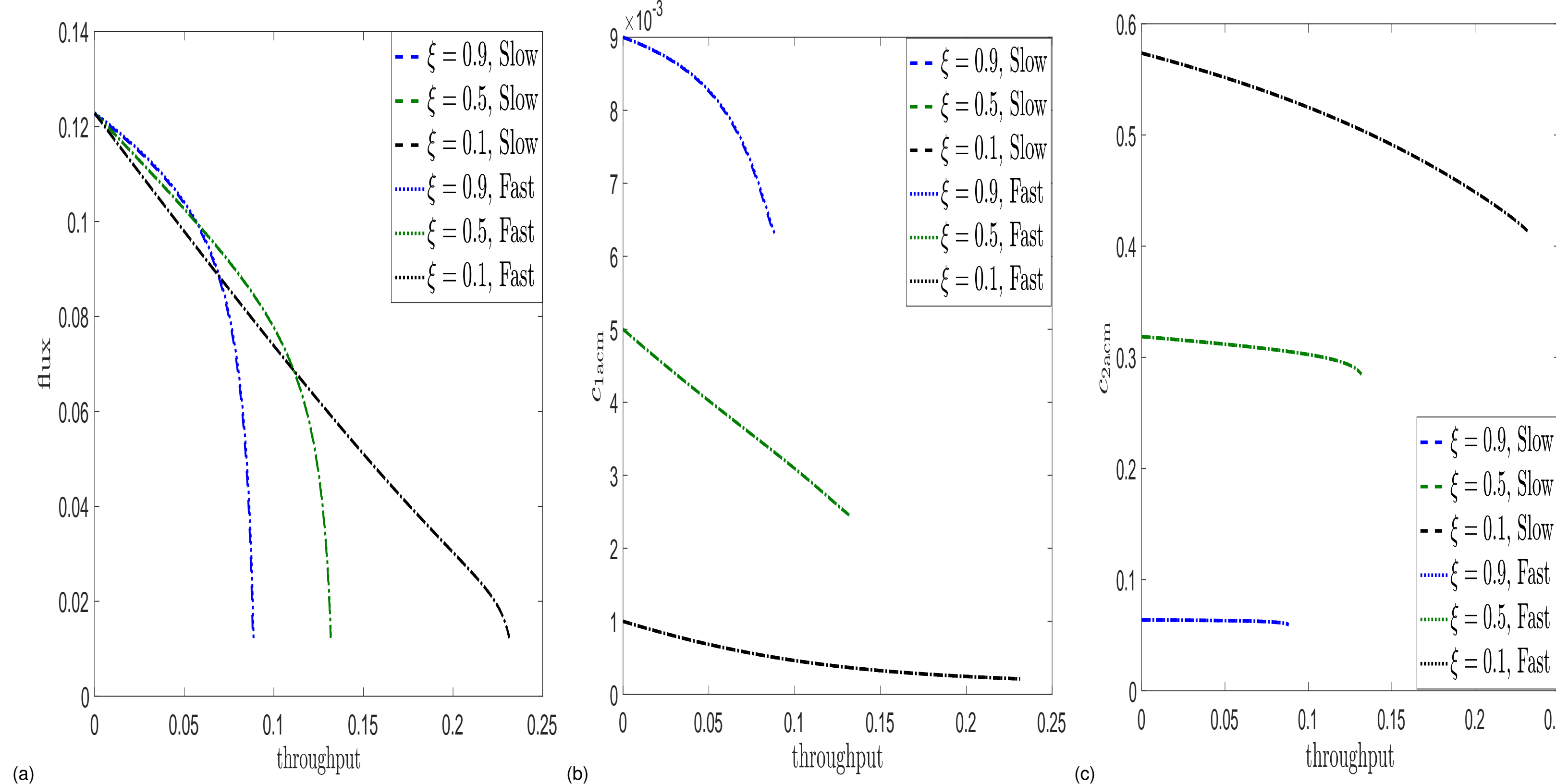


Figure 2: Comparison of slow method with objective function $J(u) = j(t_f) c_{2,acm}(t_f)$ (dashed curves) and fast method $J_{2,fast}(u) = u(0) c_{2,acm}(0)$ (dotted curves) (a-c): with $\xi = 0.9, 0.5, 0.1$ and $\beta = 0.1, \alpha_1 = \alpha_2, \lambda_1 = 1, R = 0.99$: (a) (u, j) plot, (b) $(c_{1,acm}, j)$ plot, (c) $(c_{2,acm}, j)$ plot.

For feed containing more undesirable particles, indicated by higher ξ value, the optimized pore will close faster, leading to low total throughput. We also note here the fast method finds same optimizer as slow method, with much less computation time.

3.3 Multi-stage filtration protocol

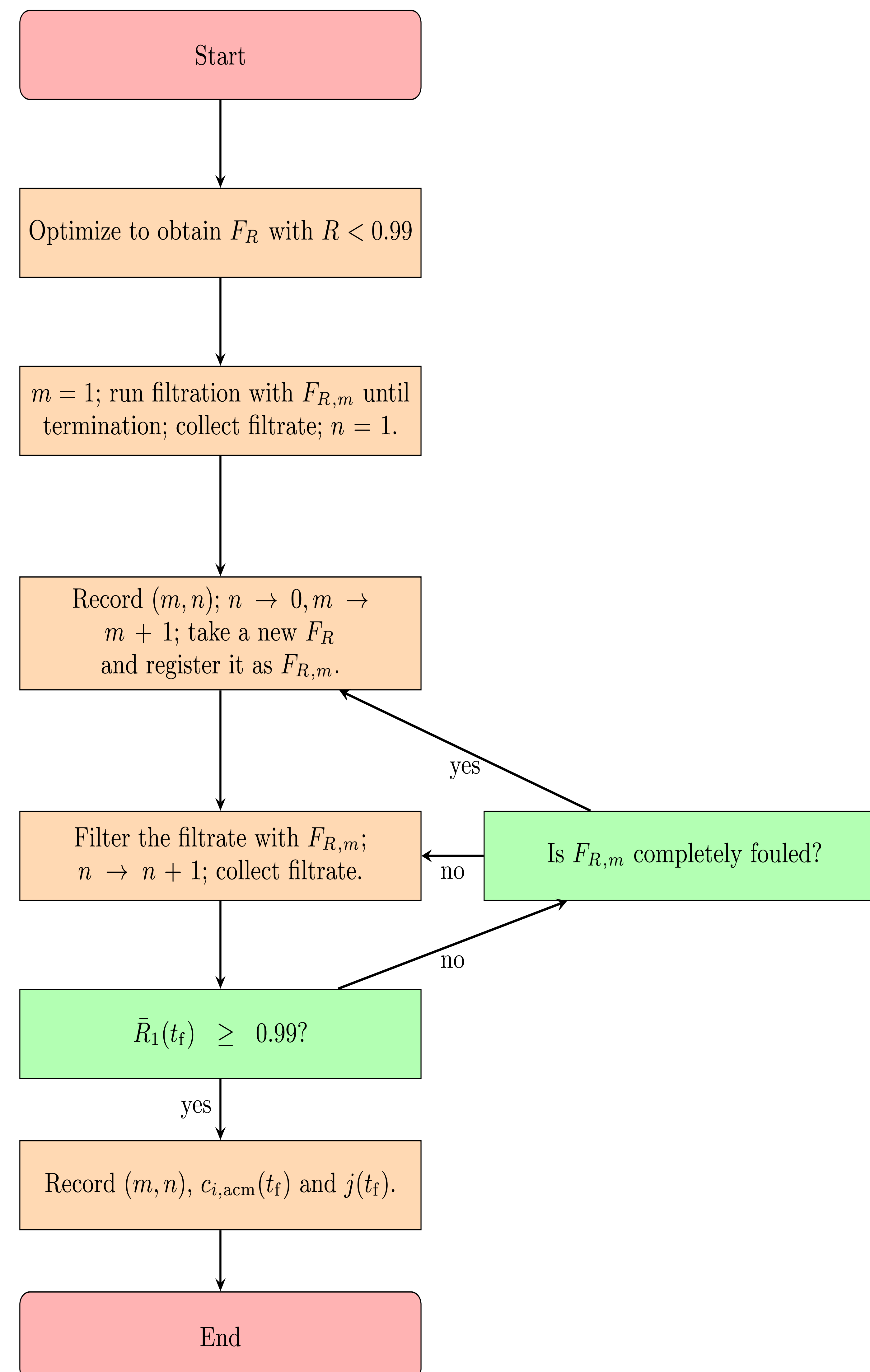


Figure 3: Flow chart of multi-stage filtration. $F_{R,m}$ signifies the m th stage filter used; for each $F_{R,m}$, $n(m)$ records how many times the filter is used.

3.4 Example of two-stage and three-stage filtrations

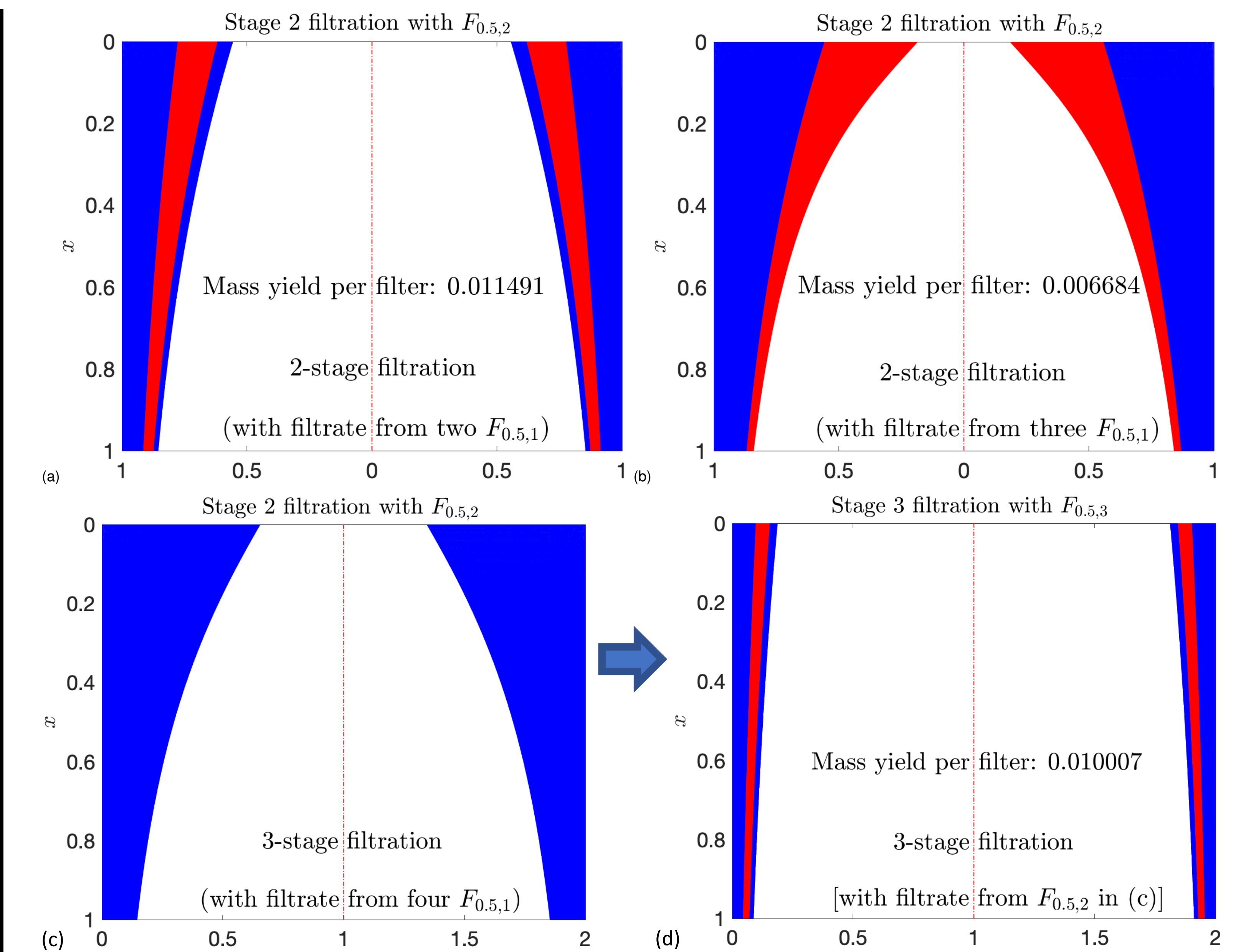


Figure 4: Multi-stage filtrations: (a, b) show second stage of 2-stage filtrations; (c, d) show 2nd and 3rd stages of a 3-stage filtration. (a) fouling of $F_{0.5,2}$ by filtering filtrate collected from two $F_{0.5,1}$ filters. (b) fouling of $F_{0.5,2}$ by filtering filtrate collected from three $F_{0.5,1}$ filters. (c) and (d): 3-stage filtration with (c) fouling of $F_{0.5,2}$ by filtering filtrate collected from four $F_{0.5,1}$ filters; (d) fouling of $F_{0.5,3}$ by filtering filtrate collected from $F_{0.5,2}$ shown in (c).

3.5 Multi-stage filtration stage-filter ratio optimization

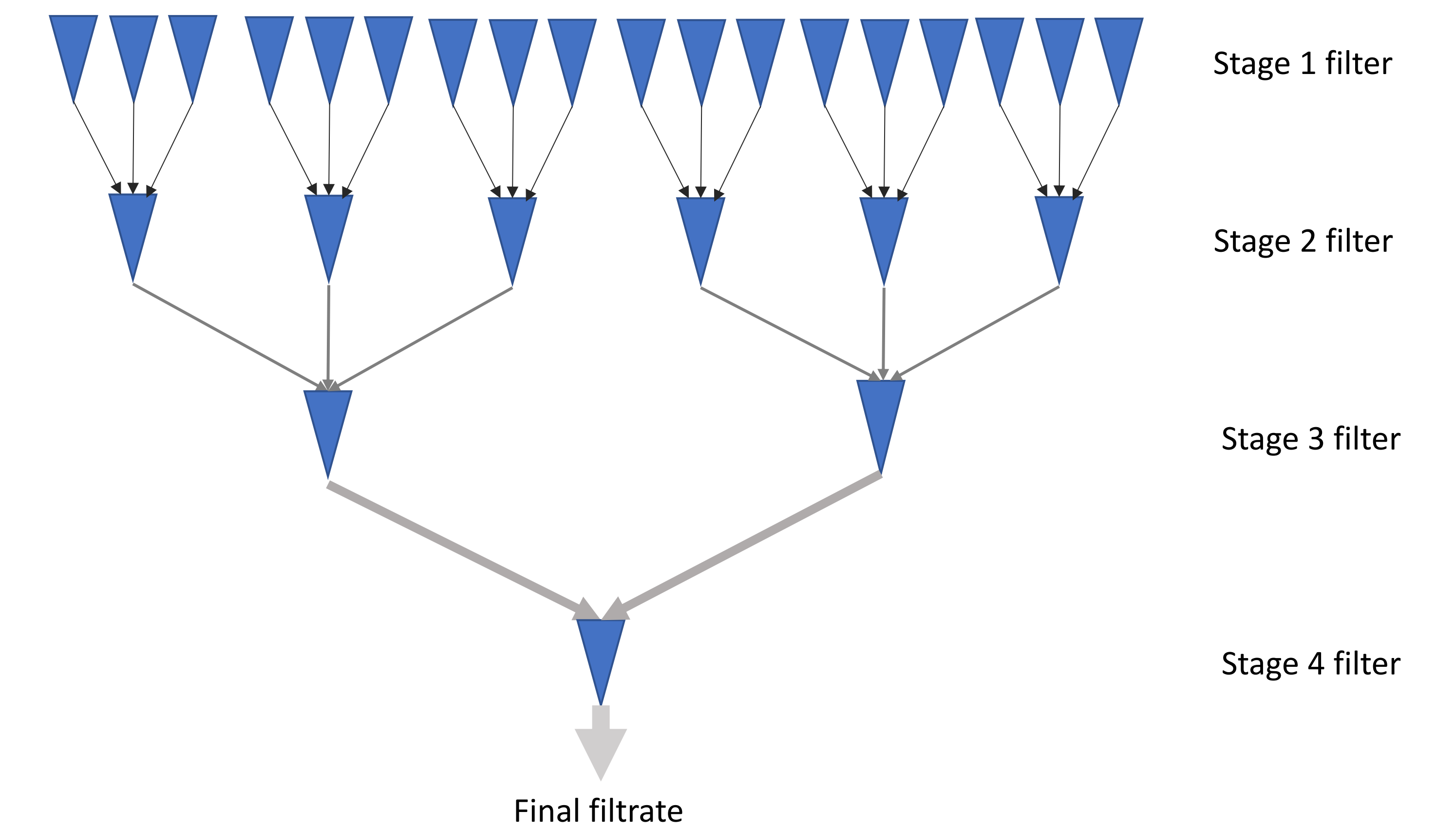


Figure 5: 4-stage filtration illustration, with eighteen stage 1 filters, six stage 2 filters, two stage 3 filters and one stage 4 filter.

4. Conclusions

- In this work we proposed a mathematical model for filtration of feed containing multiple species of particles.
- Optimization problems for maximizing the mass yield of desirable particles from feed while achieving effective separation are considered.
- For constant pressure case, we find the optimized pore profile is of 'V' shape, which is in agreement with our earlier findings [1].
- We proposed new objective function (fast method) based on the quantities evaluated at early stage of the filtration, which is 100 times faster than our earlier optimization routing (slow method).
- We proposed an alternative approach for maximizing the mass yield per filter while achieving effective separation, using multi-stage filtration.
- We find the mass yield per filter, using multi-stage filtration, could go up to two and half times of that produced by the single stage filtration, and surprisingly higher purity as well.

5. Acknowledgements

The authors acknowledge financial support from the NSF under grant DMS-1615719.

References

[1] SUN, Y. X., SANAIEI, P., KONDIS, L., CUMMINGS, L. J. Modeling and design optimization for pleated membrane filters. *Phys. Rev. Fluids* **5**, 044306 (2020).
 [2] SANAIEI, P., CUMMINGS, L. J. Flow and fouling in membrane filters: effects of membrane morphology. *J. Fluid Mech.* **818**, 744-771 (2017).
 [3] SANAIEI, P., CUMMINGS, L. J. Membrane filtration with complex branching pore morphology. *Phys. Rev. Fluids* **3**, 094305 (2018).
 [4] SUN, Y. X., KONDIS, L., CUMMINGS, L. J. Filtration with multiple species of particles. *arXiv* (to appear June 2021).